Stability Enhancement of Inverters in Grid-Connected Microgrids Using FIR Filter

Akhavan, Ali; Golestan, Saeed; Vasquez, Juan C.; Guerrero, Josep M.; Xie, Chuan

Published in:
IEEE Journal of Emerging and Selected Topics in Industrial Electronics

DOI (link to publication from Publisher):
10.1109/JESTIE.2020.3041701

Publication date:
2021

Document Version
Accepted author manuscript, peer reviewed version

This article has been accepted for publication in a future issue of this journal, but has not been fully edited. Content may change prior to final publication. Citation information: DOI 10.1109/JESTIE.2020.3041701, IEEE Journal of Emerging and Selected Topics in Industrial Electronics

Stability Enhancement of Inverters in Grid-Connected Microgrids Using FIR Filter

Ali Akhavan, *Member, IEEE*, Saeed Golestan, *Senior Member, IEEE*, Juan C. Vasquez, *Senior Member, IEEE*, Josep M. Guerrero, *Fellow, IEEE*, and Chuan Xie, *Senior Member, IEEE*

***Abstract*- Under weak grid conditions and in microgrids, the gird impedance is often large and has a highly varying nature. In such a scenario, stabilizing grid-connected inverters with an *LCL* output filter could be a challenging task. The control delay that comes from sampling and PWM may contribute to worsen this condition. Especially, the mentioned delay causes a critical frequency at one-sixth of the sampling frequency (f_s/6), which may jeopardize the converter's stability in the case of grid impedance variations. Also, the coupling effect among parallel converters, which is a likely scenario in microgrid applications, is another factor that may threaten the system stability. To deal with these challenges, this paper proposes an *LCL* filter resonance damping method that employs a finite-impulse response (FIR) filter to amend the delay effect. In this way, the system robustness is enhanced and the system keeps its stability irrespective of grid impedance variations and interaction between inverters. Experimental results show the correctness of the theoretical conclusions and confirm the efficiency of the suggested technique.**

***Index Terms*—Delay compensation, FIR filter, grid-connected inverters, *LCL* filter, microgrid, stability.**

I. INTRODUCTION

Inverters as a key element in grid-connected microgrids have been extensively used for interfacing the renewable-energy-based resources to the grid. An *LCL* filter is commonly used for attenuating switching harmonics because of its high efficiency and its low cost and size in comparison with other types of filters [1]. However, the inherent resonance of the *LCL* filter may jeopardize the system stability. Therefore, employing a resonance damping approach is necessary for the stable operation of the inverter [2]. To this end, passive and active damping methods can be employed. Basically, passive damping methods cause additional power loss, and therefore, a low efficiency [3]. Consequently, using the active damping method has received more attention [4]–[8]. However, the delay that comes from sampling and PWM may adversely affect the performance of the active damping loop [9].

Supposing T_s as the sampling period and considering the total delay in the control loop equal to $1.5T_s$, the virtual impedance corresponding to resonance mitigation behaves as a negative resistance at frequencies higher than one-sixth of the sampling frequency (f_s/6), so-called critical frequency [10]. Therefore, the conventional active damping methods not only have no positive effect on the system stability, but also might make the system unstable in a case that the resonance occurs at frequencies higher than f_s/6. It implies that the system is at the risk of instability in a weak grid, where the grid impedance and consequently, the resonance frequency change in a wide range. The situation may become worse in a microgrid where the interaction between parallel converters changes the grid impedance seen by each inverter [11], [12]. Therefore, the conventional active damping methods should be modified to expand the critical frequency and increase the system robustness against the above-mentioned non-idealities. To this end, the delay should be taken into account to compensate for its adverse effect.

Extensive research works have been done to amend the adverse effect of the delay. A high-pass filter (HPF) is proposed in [13] to introduce a phase lead to the system and in this way, it compensates for the phase lag caused by the delay. Although effective, the HPF may amplify high-frequency noises depending on its crossover frequency. A similar idea is proposed in [14], where a reciprocal of a notch filter is employed. However, it only expands the effective active damping area up to f_s/4, which might not be sufficient in the case of wide grid impedance variations. A biquad filter is proposed in [15] for expanding the critical frequency. However, its parameters tuning and implementation are not straightforward. Li *et al.* [16] proposed a repetitive-based approach to improve the system performance. Nevertheless, this method may increase noises at the Nyquist frequency because of its infinite gain at this frequency. An observer is employed in [17] to predict the capacitor current and amend the delay. However, this method has a high sensitivity to uncertainties and parameters mismatch.

Although effective, almost all the above-mentioned methods complicate the control system and demand additional computational effort. To overcome the phase lag caused by the delay and expanding the critical frequency without considerably complicate the control structure, this paper presents a new approach to amend the adverse delay effect based on a finite-impulse response (FIR) filter. FIR filters

Manuscript received July 7, 2020; revised October 10, 2020; accepted November 22, 2020. This work was supported in part by VILLUM FONDEN under the VILLUM Investigator Grant (no. 25920): Center for Research on Microgrids (CROM), and in part by the National Natural Science Foundation of China under Grant 51807021.

A. Akhavan, S. Golestan, J. C. Vasquez, and J. M. Guerrero are with the Department of Energy Technology, Aalborg University, 9220 Aalborg, Denmark (e-mail: alak@et.aau.dk; sgd@et.aau.dk; juq@et.aau.dk; joz@et.aau.dk).

Chuan Xie is with the School of Automation Engineering, University of Electronic Science and Technology of China, Chengdu 611731, China (e-mail: c.xie@uestc.edu.cn).

This article has been accepted for publication in a future issue of this journal, but has not been fully edited. Content may change prior to final publication. Citation information: DOI 10.1109/JESTIE.2020.3041701, IEEE Journal of Emerging and Selected Topics in Industrial Electronics

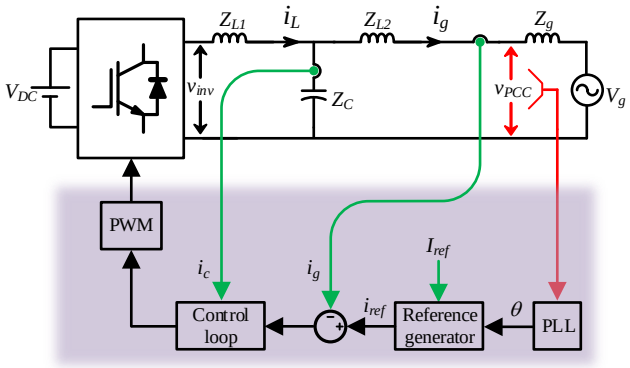

Fig. 1. Single-line scheme of a three-phase current-controlled inverter.

belong to the digital filter family, which the main characteristic of them is the ease of implementation. In addition, the filter coefficients could be regarded as a degree of freedom to achieve the desired phase-magnitude characteristic. FIR filters are frequently used in designing repetitive controllers for power quality enhancement [18], [19]. However, to the best knowledge of authors, this type of filter has not been used for the stability enhancement of grid-connected inverters. This paper employs an FIR filter to modify the conventional active damping control method. The proposed approach is robust against grid impedance variations and coupling effects among inverters in a microgrid.

This paper first presents an overall system description in Section II. In Section III, a new FIR-based delay compensation method is presented. The system stability is investigated in Section IV in the case of grid impedance variations and coupling effect among inverters. Section V is devoted to the experimental validation of the suggested technique in different case studies. Finally, the paper is concluded in Section VI.

II. System Modeling

Fig. 1 illustrates the single-line diagram of a three-phase grid-connected inverter, in which Z_{L1}, Z_{L2}, Z_C, and Z_g (see (1)) are the impedances corresponding to the inverter-side and grid-side inductors, filter capacitor, and grid line inductance, respectively:

$$Z_{L1} = L_1 s,\ Z_{L2} = L_2 s,\ Z_C = \frac{1}{Cs},\ Z_g = L_g s\ . \tag{1}$$

Per-phase control block diagram of a current-controlled grid-connected inverter that regulates the grid-side current is presented in the z-domain in Fig. 2. In this figure, the sampling delay is modeled as z^{-1}. Also, the PWM effect can be modeled with the zero-order-hold (ZOH) transfer function [20]

$$G_{ZOH}(s) = \frac{1 - e^{-sT_s}}{s}. \tag{2}$$

$G_i(z)$ is the current controller. Also, $K_{PWM} = V_{DC}/(2\,V_{tri})$ is the inverter's transfer function, where V_{tri} and V_{DC} are the amplitude of the triangular carrier and DC-link voltage, respectively. The capacitor current i_c is passed through the active damping controller $G_{ad}(z)$ to mitigate the resonance of the *LCL* filter. By rearranging Fig. 2 using block diagram algebra, Fig. 3 can be obtained. This representation, which is depicted in s-domain for the sake of simplicity, shows that the capacitor current-based active damping builds a virtual impedance in parallel with the filter capacitor as [10]

$$Z_{ad}(s) = \frac{L_1}{CK_{PWM}G_{ad}(s)G_d(s)} \tag{3}$$

where $G_d(s)$ is the aggregated model of the PWM and computational delays.

$$G_d(s) = e^{-1.5T_s s} \tag{4}$$

A proportional controller is basically used in the conventional active damping methods. Supposing $G_{ad}(s) = K_{ad}$, the virtual impedance can be represented as follows:

$$Z_{ad}(j\omega) = \frac{L_1}{CK_{PWM}K_{ad}}\left[\cos(1.5\omega T_s) + j\sin(1.5\omega T_s)\right]. \tag{5}$$

From (5), it could be easily found that the real part of Z_{ad} has a positive value within (0, f_s/6), and has a negative value within (f_s/6, f_s/2). In other words, it looks like a negative resistance in the interval of (f_s/6, f_s/2). Therefore, when the resonance occurs in the negative resistance area, the conventional active damping method not only has no positive effect on the system stability, but also impairs the system stability. Thus, the delay effect may threaten the stable operation of inverters, especially in weak grids, where the grid impedance varies in a wide range and therefore, changes the resonance frequency. To enhance the robustness of inverters against the grid impedance variations, the positive area of the virtual resistance should be widened. From (3), the active damping controller could be designed to amend the delay effect.

III. Stability Enhancement Using FIR Filter

The main purpose of this section is to compensate for the delay effect. However, the reciprocal of $G_d(s)$ is not casual and cannot be implemented in practice. Therefore, an FIR filter is used to approximate the behavior of the reciprocal of the delay transfer function, i.e., $1/G_d(s)$.

A. FIR Filter Overview

FIR filters belong to the digital filter family whose impulse response settles down to zero in a finite number of sample intervals [18]. The structure of an N-order FIR filter is depicted in Fig. 4, where comprises N delay taps and $N + 1$ weight coefficients. FIR filters are always stable and their implementation is easy [21]. The transfer function of a typical FIR filter is given by

$$H(z) = \frac{W(z)}{R(z)} = a_0 + a_1 z^{-1} + a_2 z^{-2} + \cdots + a_{N-1} z^{N-1} + a_N z^{-N}. \tag{6}$$

A high-order FIR filter ensures an accurate phase-magnitude characteristic, but it needs more computational effort. Therefore, one needs to make a trade-off decision between the accuracy and computational burden. In this paper, a 10th-order (N = 10) FIR filter is used for the delay

This article has been accepted for publication in a future issue of this journal, but has not been fully edited. Content may change prior to final publication. Citation information: DOI 10.1109/JESTIE.2020.3041701, IEEE Journal of Emerging and Selected Topics in Industrial Electronics

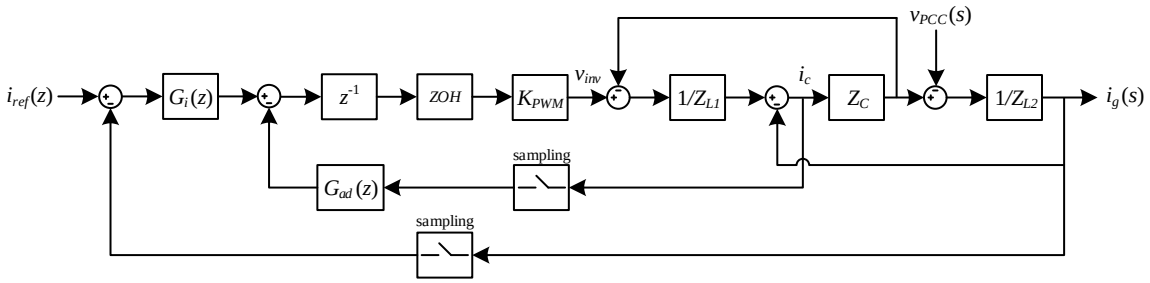

Fig. 2. Control scheme of the current-controlled grid-connected inverter.

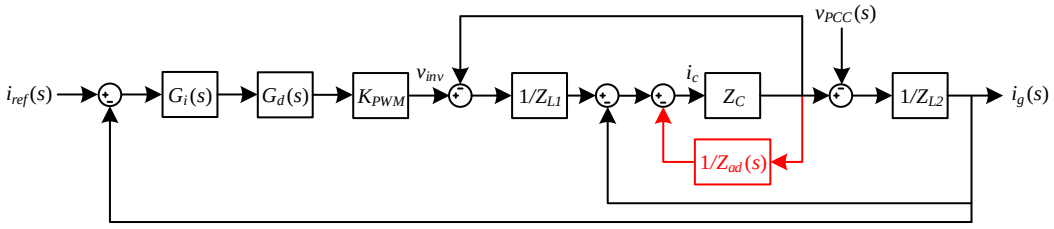

Fig. 3. Mathematically equivalent block diagram of Fig. 2 in *s*-domain.

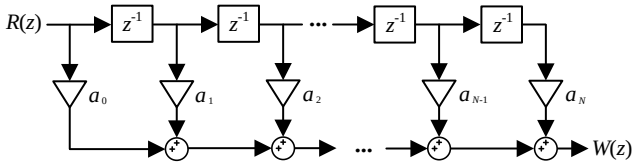

Fig. 4. Structure of the FIR filter.

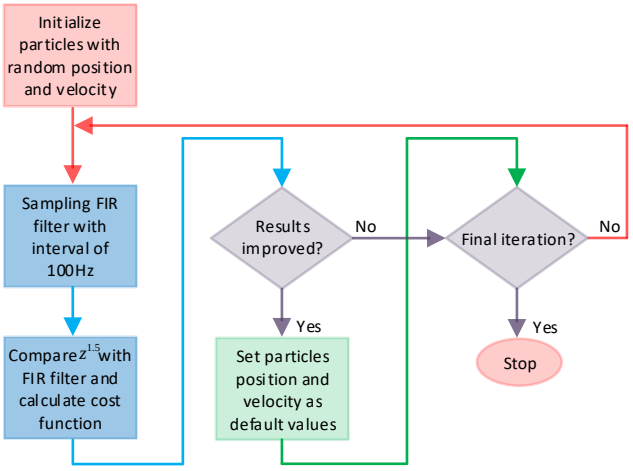

Fig. 5. Flowchart of PSO algorithm.

compensation. The coefficients of the FIR filter should be designed to mimic the desired transfer function $z^{1.5}$. To this end, a particle swarm optimization (PSO) algorithm is used for tuning the coefficients. The cost function (*CF*) comprises of the error between magnitude and phase of the desired transfer function ($z^{1.5}$) and FIR filter ($H(z)$), i.e.,

$$CF = \left\| z^{1.5} \right| - \left| H(z) \right\| + \left| \angle z^{1.5} - \angle H(z) \right|. \quad (7)$$

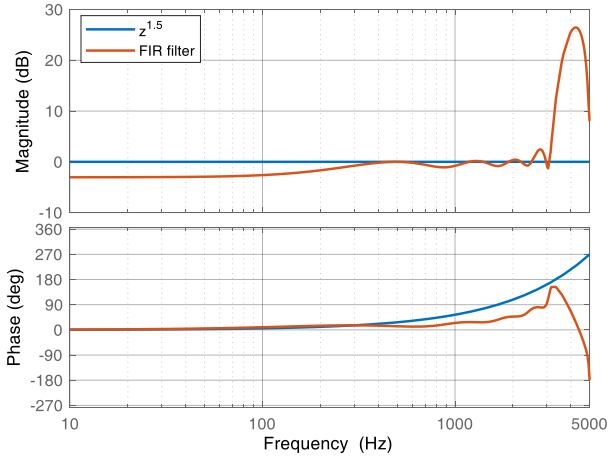

Fig. 6. Bode plots of $z^{1.5}$ and the FIR filter designed by PSO.

TABLE I
FIR Filter Coefficients

a_0 = 2.2675	a_1 = -3.1968	a_2 = 3.4947	a_3 = -2.5123
a_4 = 0.3715	a_5 = 1.9278	a_6 = -3.5380	a_7 = 3.7991
a_8 = -2.9589	a_9 = 1.5916	a_{10} = -0.5419	

The flowchart of the PSO algorithm is illustrated in Fig. 5 and its related parameters are presented in the Appendix. The PSO algorithm is well-known and its details are out of the scope of this paper. More details could be found in [22]–[24]. The coefficients of $H(z)$ derived from PSO is presented in Table I. Fig. 6 depicts the Bode plot of $H(z)$ and $z^{1.5}$ for the sake of comparison. As shown in this figure, the FIR filter introduces a positive phase to the control system up to 4500 Hz. Therefore, it can help to amend the negative phase caused by the delay and thus, expand the critical frequency. The Bode plots of virtual impedance supposing $G_{ad} = K_{ad}$ and $G_{ad} = H(z)$

This article has been accepted for publication in a future issue of this journal, but has not been fully edited. Content may change prior to final publication. Citation information: DOI 10.1109/JESTIE.2020.3041701, IEEE Journal of Emerging and Selected Topics in Industrial Electronics

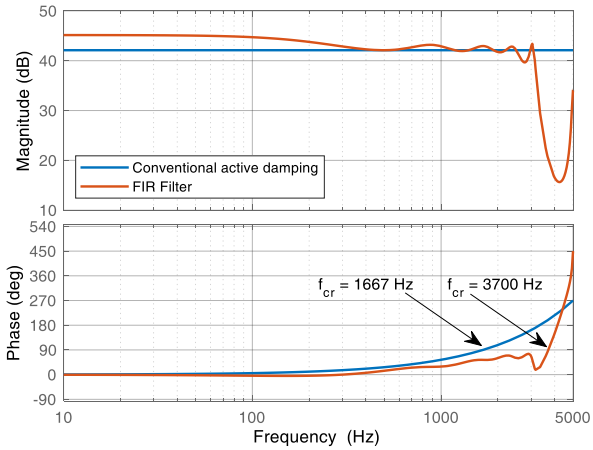

Fig. 7. The Bode plot of virtual impedance using the conventional and FIR-based active damping.

are shown in Fig. 7. It is clear that in the case of conventional active damping, in which a proportional controller is used, the real part of $Z_{ad}(s)$ is positive only up to $f_s/6$ = 1667 Hz (where the phase curve passes 90°). However, by using the FIR filter, the positive region of the virtual impedance is expanded up to 3700 Hz.

The above observation shows that the FIR filter can expand the critical frequency, which in turn, expands the effective active damping region. Thus, it enhances the system robustness and improves the system stability against the grid impedance and resonance frequency variations.

B. Tuning Parameters

A proportional-resonant (PR) regulator in the $\alpha\beta$ frame could be employed as the current controller, as expressed below:

$$G_i(s) = k_p + \frac{k_r s}{s^2 + 2\omega_i s + \omega_o^2} \tag{8}$$

where $\omega_o = 2\pi f_o$, f_o is the fundamental frequency, and $\omega_i = \pi$ is the cut-off frequency of the regulator.

Tuning the proportional gain k_p is based on the desired crossover frequency f_c and, therefore, could be designed as [25]

$$k_p = \frac{2\pi f_c (L_1 + L_2)}{K_{PWM}} \tag{9}$$

where f_c is selected 0.05 f_s [26], [27]. The corner frequency of the PR controller i.e., $k_r/(2\pi k_p)$, is usually set as $0.1f_c$ to reduce the phase contribution at the crossover frequency [28]. Therefore, the resonant controller could be selected as

$$k_r = \frac{2\pi f_c}{10} k_p \,. \tag{10}$$

TABLE II
System Parameters

DC-link voltage, V_{DC}	650 V
Inverter-side inductor, L_1	8.6 mH
Filter capacitor, C	4.5 µF
Grid-side inductor, L_2	1.8 mH
Sampling frequency	10 kHz
Rated power of inverter	2.2 kVA
Grid voltage, V_g	400 V (Line to line)
Frequency	50 Hz
Grid inductance, L_g	$0 < L_g < 20$ mH

TABLE III
Control Parameters

k_p	30
k_r	5000
K_{ad}	15
V_{tri}	$V_{DC}/2$
K_{PWM}	1

From (9), (10), and also using the parameters listed in Table II, k_p = 30 and k_r = 5000 are achieved. Finally, the discrete form of the current controller can be obtained as follows [29]:

$$G_i(z) = k_p + k_r \frac{T_s(z-1)}{z^2 + z(\omega_o^2 T_s^2 + 2\omega_i T - 2) - 2\omega_i T_s + 1}. \tag{11}$$

The magnitude of virtual impedance should be designed to mitigate the resonance. From (3), manipulating the active damping controller is the soundest choice for tuning the magnitude of virtual impedance. Therefore, the transfer function $G_{ad}(z)$ could be presented as

$$G_{ad}(z) = K_{ad} H(z) \tag{12}$$

where K_{ad} is the gain of the FIR filter. It is worthy to note that K_{ad} does not have any contribution to the phase compensation, and it could be solely used for the resonance mitigation. Through numerous simulations, it is found that a 70 Ω virtual resistor paralleled with the filter capacitor is suitable for the mitigation of the resonance. By solving (3) in resonance frequency, K_{ad} = 15 is achieved.

IV. Stability Investigation

In this section, the system stability and its robustness are investigated under different conditions.

A. Stability Investigation Against Grid Impedance Variations

To investigate the stability of grid injected current i_g with the conventional and proposed methods, the loop gain of the control system is obtained using Fig. 2 in z-domain as (13) at the bottom of this page. Fig. 8(a) shows the poles of the closed-loop transfer function relating the reference current to

$$T_{g\_ff}(z) = \frac{G_i(z)K_{PWM}}{\omega_r(L_1+L_2+L_g)} \cdot \frac{\omega_r T_s(z^2 - 2z\cos(\omega_r T_s) + 1) + (z-1)^2 \sin(\omega_r T_s)}{z(z-1)(z^2 - 2z\cos(\omega_r T_s) + 1) + K_w G_i(z) \frac{K_{PWM}\sin(\omega_r T_s)}{\omega_r L_1}(z-1)^2 - G_{ff}(s)\frac{L_g K_{PWM}}{L_1+L_2+L_g}(1-\cos(\omega_r T_s))(z^2-1)} \tag{13}$$

This article has been accepted for publication in a future issue of this journal, but has not been fully edited. Content may change prior to final publication. Citation information: DOI 10.1109/JESTIE.2020.3041701, IEEE Journal of Emerging and Selected Topics in Industrial Electronics

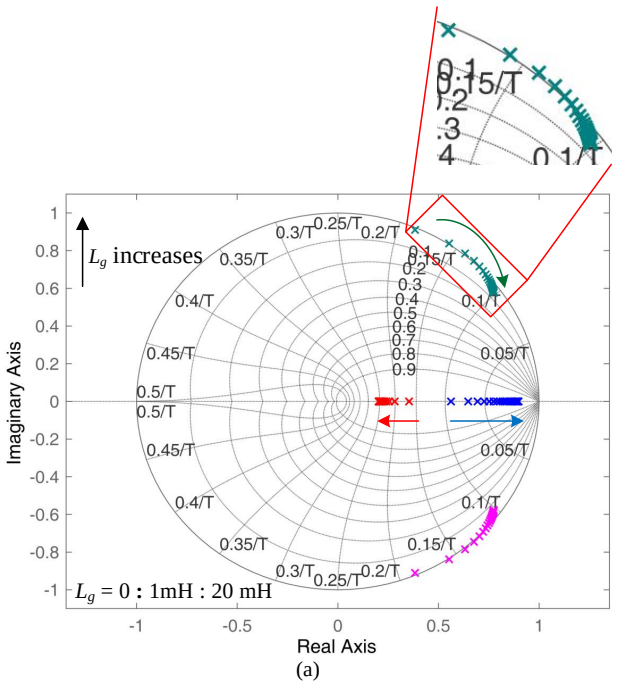

Fig. 8. Closed-loop poles movement of the control system. (a) Conventional active damping method. (b) FIR-based active damping method.

the output current, $T_g(z)/[1+ T_g(z)]$ using the conventional method (supposing $G_{ad}(s) = K_{ad}$), with L_g varying up to 20 mH and using parameters listed in Tables II and III. As Fig. 8(a) shows, when $L_g = 0$, the system is stable since the closed-loop poles are located within the unit circuit. However, for $L_g > 0$, the resonant poles move to the unstable region and then come back inside the unit circle with a further increase of L_g. It proves that the conventional active damping control method has a poor robustness against the grid impedance variations.

The closed-loop poles movement of the proposed control system is depicted in Fig. 8(b). Note that because of using the FIR filter, the number of poles is higher compared to the previous case. As shown, the closed-loop poles remain inside the unit circuit, irrespective of grid impedance wide variations,

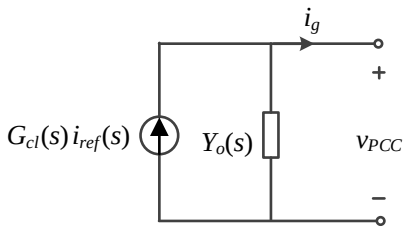

Fig. 9. Norton equivalent circuit of the current-controlled inverter.

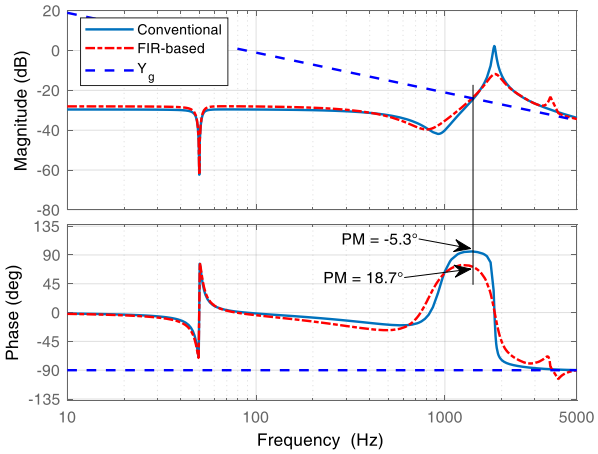

Fig. 10. The Bode diagrams of Y_o with conventional and FIR-based active damping methods as well as grid admittance Y_g.

which means the system robustness is enhanced significantly thanks to the FIR filter.

Fig. 9 illustrates the Norton equivalent circuit of a current-controlled inverter. In this figure, $G_{cl}(s)$ is the system closed-loop transfer function. Also, $Y_o(s)$ is the inverter output admittance, which could be used for the stability investigation. For the sake of generality, $Y_o(s)$ is derived using Fig. 3 as (14), for stability examination of the inverter under different grid impedance.

$$Y_o(s) = \left.\frac{i_g(s)}{-v_{PCC}(s)}\right|_{i_{ref}=0} = \frac{s^2 L_1 C + 1 + sCG_{ad}G_d}{s^3 L_1 L_2 C + s(L_1 + L_2) + k_p G_d + s^2 L_2 C G_{ad} G_d} \tag{14}$$

The Bode diagrams of $Y_o(s)$ using the FIR controller, as well as the conventional active damping control method (supposing $G_{ad} = K_{ad}$) and the Bode diagram of grid admittance for L_g = 1.8 mH are depicted in Fig. 10. To ensure about the stable operation of two paralleled subsystems, the output admittance of those subsystems must have a positive phase margin where their Bode diagrams intersect at the frequency f_i, [30], i.e.

$$\mathrm{PM} = 180° - [\angle Y_o(f_i) - \angle Y_g(f_i)]\,. \tag{15}$$

As it could be seen in Fig. 10, using the conventional control system, $Y_o(s)$ intersects with $Y_g(s)$ where the PM is negative, which will cause instability. On the other hand, the PM is always positive at the intersection point by using the

This article has been accepted for publication in a future issue of this journal, but has not been fully edited. Content may change prior to final publication. Citation information: DOI 10.1109/JESTIE.2020.3041701, IEEE Journal of Emerging and Selected Topics in Industrial Electronics

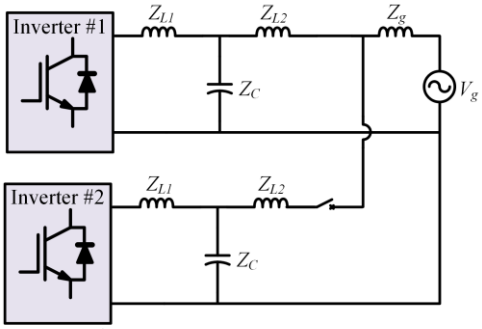

Fig. 11. Structure of two paralleled inverters.

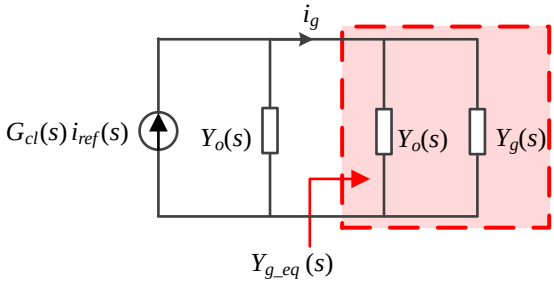

Fig. 12. The equivalent impedance schematic model for two paralleled inverters.

FIR controller since the phase of $Y_o(s)$ is lower than 90°. Fig. 10 proves again that the system robustness against the grid impedance variations is enhanced.

B. Stability Investigation in Multi-paralleled systems

In a microgrid, paralleled converters have a coupling effect that changes the equivalent grid admittance seen by each inverter [11]. Therefore, in addition to the grid admittance, the parallel connection of inverters can put the system at the risk of instability. To investigate the robustness of the control system in multi-paralleled systems, the interconnection of two inverters as shown in Fig. 11 is investigated. The physical and control parameters of inverters are supposed to be the same. Also, L_g = 0.5 mH is selected for this study. By substituting the Norton equivalent circuit in Fig. 9 instead of inverters in Fig. 11, the equivalent model of paralleled inverters could be obtained as shown in Fig. 12. It is worthy to note that in the depicted figure, the inverter's equivalent current source and grid voltage are supposed to be zero because they do not change the equivalent grid admittance (Y_{g_eq}) that is seen by each inverter. From Fig. 12, $Y_{g\_eq}(s) = Y_o(s) + Y_g(s)$ could be achieved. Therefore, for the investigation of stability in a multi-paralleled system, Y_{g_eq} should be investigated instead of Y_g.

Fig. 13 shows the Bode diagrams of $Y_o(s)$ using the conventional active damping method, the equivalent grid admittance Y_{g_eq} and grid admittance corresponding to a case in which only one inverter is connected to the grid (L_g = 0.5 mH). It could be seen that $Y_o(s)$ and $Y_g(s)$ intersect where the system has a positive PM (PM = 7.4°) which shows the connection of a single inverter to the grid is stable. However, in the case that both inverters are connected, the PM becomes negative (PM = -5.2°). It means that the interconnection of two inverters makes the system unstable.

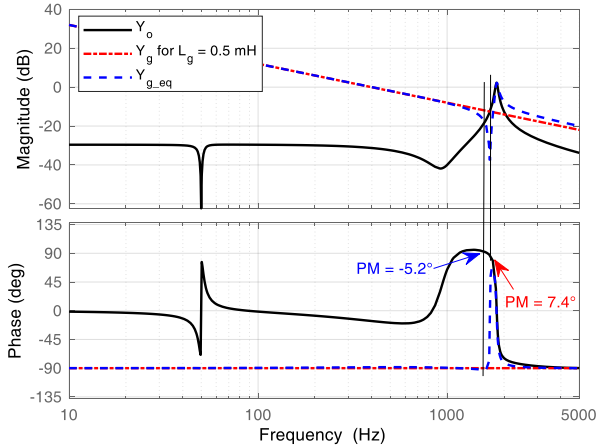

Fig. 13. The Bode diagrams of Y_o, Y_g, and Y_{g_eq} using the conventional active damping method.

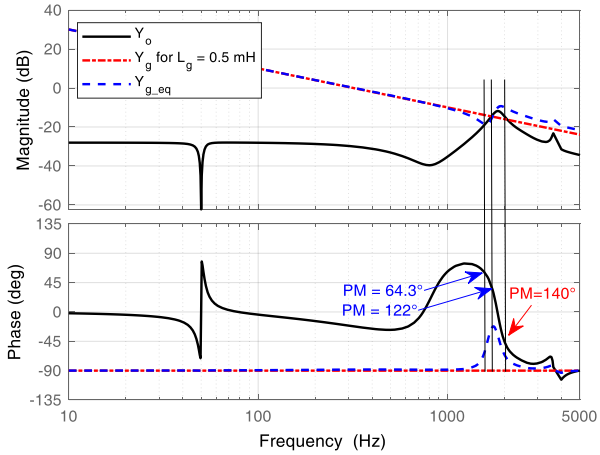

Fig. 14. The Bode diagrams of Y_o, Y_g, and Y_{g_eq} using the FIR-based active damping method.

Fig. 15. Experimental setup.

To confirm the capability of the FIR-based active damping method, an investigation is done by using the proposed method in Fig 14. It could be clearly seen that the system has a positive PM at the intersection points either in the case of connection of a single or two grid-connected inverters. The analytical results show that the system keeps its stability,

This article has been accepted for publication in a future issue of this journal, but has not been fully edited. Content may change prior to final publication. Citation information: DOI 10.1109/JESTIE.2020.3041701, IEEE Journal of Emerging and Selected Topics in Industrial Electronics

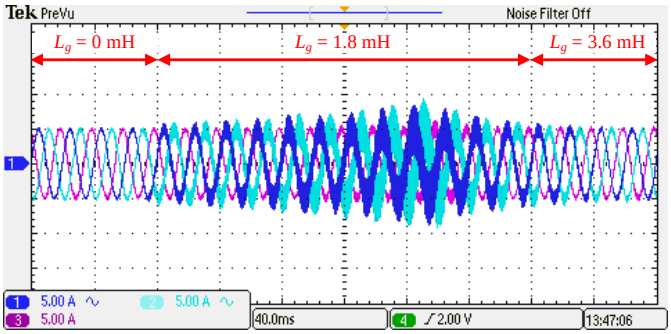

Fig. 16. Three-phase injected current to the grid with the conventional active damping method with varying grid impedance.

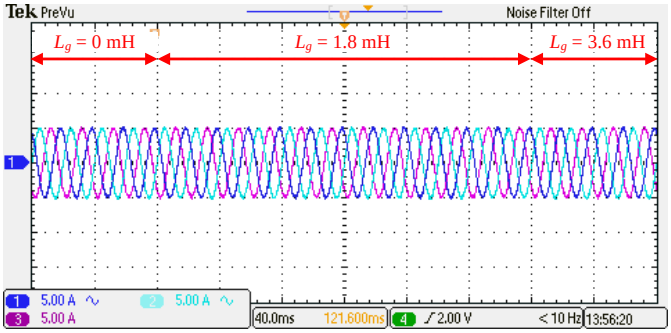

Fig. 17. Three-phase injected current to the grid with the FIR-based active damping method with varying grid impedance.

irrespective of the number of paralleled inverters. In other words, since the phase of $Y_o(s)$ is always lower than 90°, the coupling effect among inverters never makes the system unstable.

V. Experimental Results

Fig. 15 shows an experimental setup that is built up to confirm the capability of the proposed FIR-based active damping method. Two-level three-phase *Danfoss* inverters with the rating power of 2.2 kW are used. The *dSPACE* DS1006 is used for the implementation of the control system. Also, a grid-simulator *Chroma 61845* is used as an ideal grid. The physical system parameters and control ones are summarized in Table II and III, respectively.

A. Grid Impedance Variations

To show the system performance in weak grid conditions, an experiment is carried out where the grid inductance changes from 0 to 1.8 mH and then, to 3.6 mH. The output current of the inverter controlled by the conventional method is shown in Fig. 16. It can be seen that the system is stable when it is connected to a stiff grid with $L_g = 0$. However, the inverter becomes unstable when L_g increases to 1.8 mH and it again becomes stable when L_g further increases to 3.6 mH. The experimental results show the poor stability of the conventional active damping method in varying grid impedance conditions.

The experiment is repeated using the FIR controller. As shown in Fig. 17, the system keeps its stability irrespective of grid impedance variations. The experimental results in this section verify the analytical results associated with Figs. 8 and 10.

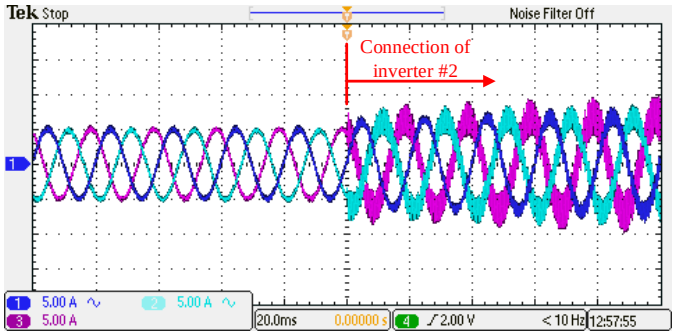

Fig. 18. The total injected current of two inverters with the conventional active damping method.

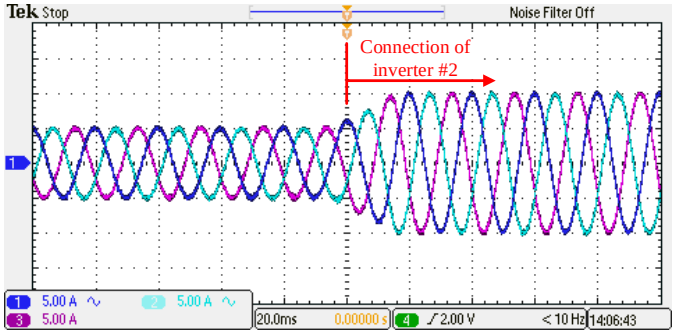

Fig. 19. The total injected current of two inverters with the FIR-based active damping method.

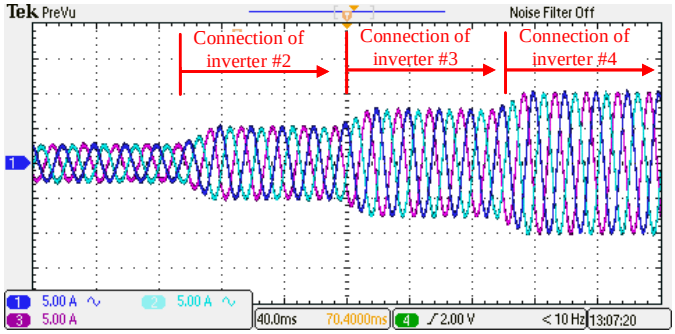

Fig. 20. The total injected current of four inverters with the FIR-based active damping method.

B. Coupling Effect among Parallel Inverters

In this part, the interconnection of two inverters is investigated to evaluate the stability of the control system in multi-paralleled systems. To do this, the first inverter is injecting the current to the grid and then, the second one is suddenly connected. The results for the case of using the conventional control system is shown in Fig. 18. As experimental results show, the system works stably at first, however, after the connection of the second inverter, the whole of the system becomes unstable. The total grid injected current for the system using the FIR controller is shown in Fig. 19. It can be seen that the system keeps its stability even after the connection of the second inverter. The experimental results verify the analytical results associated with Figs. 13 and 14, and show that the system is stable regardless of the number of parallel inverters.

For the sake of generality and verification of the control system, a parallel connection of four inverters is evaluated. To

This article has been accepted for publication in a future issue of this journal, but has not been fully edited. Content may change prior to final publication. Citation information: DOI 10.1109/JESTIE.2020.3041701, IEEE Journal of Emerging and Selected Topics in Industrial Electronics

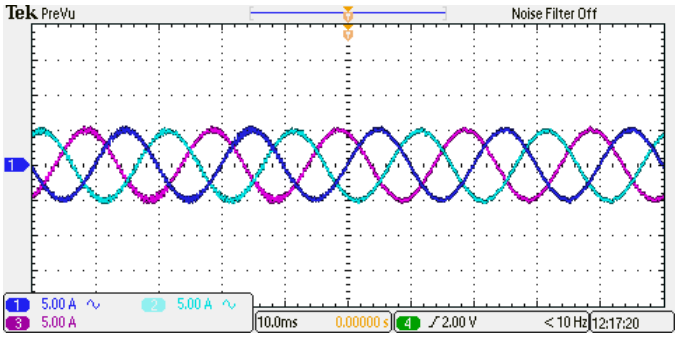

(a)

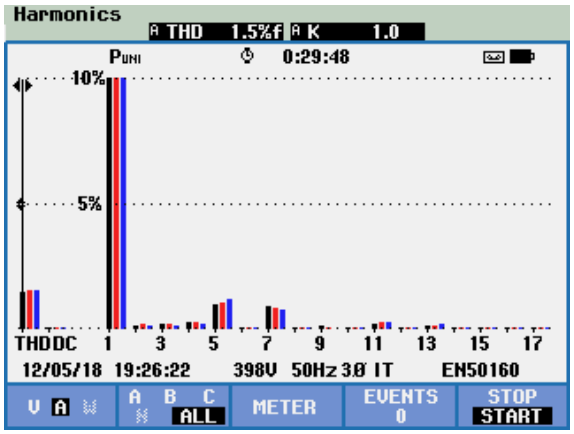

(b)

Fig. 21. The experimental results in a poor power quality condition. (a) The injected current to the grid. (b) The harmonic spectrum of the injected current.

this end, inverters are connected one by one to the grid. The total output current in this scenario is shown in Fig. 20. It could be seen that the system can work stably irrespective of the number of parallel inverters. It means that system has strong robustness against the coupling effect among inverters and, therefore, could be used in grid-connected microgrids.

C. Poor Power Quality Conditions

In this section, an experiment is carried out in a poor power quality condition, where third and fifth harmonics are added to the grid voltage using grid-simulator *Chroma*. The magnitude of these components is 5% and 3%, respectively.

The injected current to the grid and its harmonic spectrum are presented in Fig. 21. As shown, the total harmonic distortion (THD) is 1.5%, which is below limits stipulated by international standards. These results imply that the proposed control method can provide a satisfactory performance in distorted grid conditions.

D. Parallelizing Inverters with Different Parameters

In the next experiment, the connection of two inverters with different *LCL* filters is considered to show the effectiveness of the proposed method in a microgrid with different inverters. The system and control parameters of the first inverter are summarized in Table II and III, respectively. The system parameters of the second inverter are summarized in Table IV. Note that the *LCL* filter resonance frequency (f_r = 1694Hz) for this unit is higher than $f_s/6$, and therefore, it needs

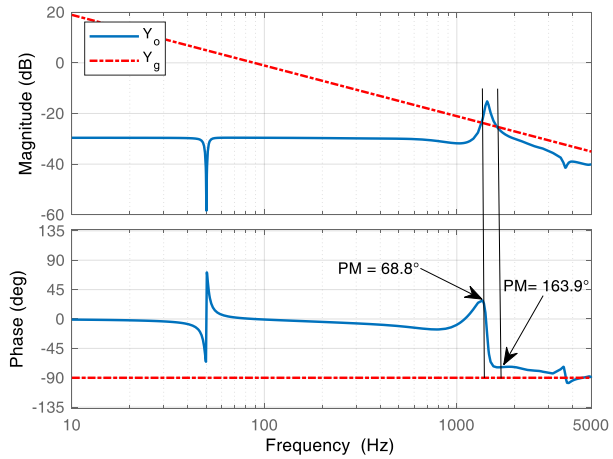

Fig. 22. The Bode diagrams of Y_o and Y_g for the inverter introduced in Section V. D.

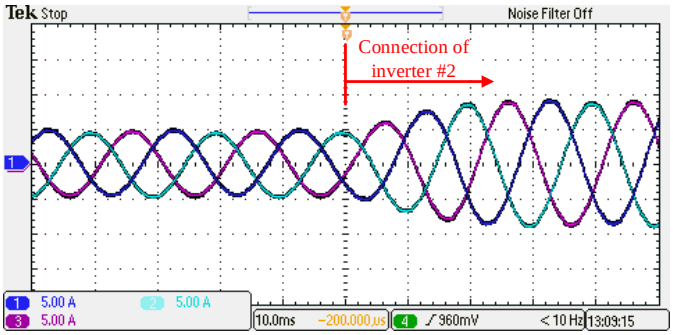

Fig. 23. The total injected current of two inverters with different parameters using the FIR-based active damping.

TABLE IV
System Parameters for Inverter #2

DC-link voltage, V_{DC}	650 V
Inverter-side inductor, L_1	4.3 mH
Filter capacitor, C	4.5 μF
Grid-side inductor, L_2	3.6 mH
Sampling frequency	10 kHz
Rated power of inverter	2.2 kVA
Grid voltage, V_g	400 V (Line to line)
Frequency	50 Hz

TABLE V
Control Parameters for Inverter #2

k_p	25
k_r	5000
K_{ad}	15
V_{tri}	$V_{DC}/2$
K_{PWM}	1

delay compensation to expand the critical frequency. The same FIR filter as that used for the inverter 1 is employed for the delay compensation here. Also, the same design guidelines as those described in Section III. B is adopted for tuning the control parameters of the inverter 2, therefore, it is not repeated here to save space. The corresponding control parameters are summarized in Table V.

The Bode diagram of the inverter output admittance (Y_o), as well as grid admittance (Y_g) for L_g = 1.8 mH are plotted in Fig. 22. As shown in this figure, the phase of Y_o is always lower than 90°, in which, shows the inverter is stable irrespective of the intersection point between Y_o and Y_g. Fig. 23 shows the experimental results when the second inverter connects after the first one. As can be observed, the system keeps its stability when inverters (which have different parameters) are connected together.

It is worth mentioning here that in interconnecting inverters with different circuit parameters, one should note that they have different *LCL* resonance frequency and critical frequency. These points should be taken into account in designing the delay compensation technique.

VI. Conclusion

An improved active damping method using FIR filters for stability enhancement of grid-connected inverters in weak grids is presented in this paper. It is shown that grid impedance variations may impair the system stability due to the delay effect in the conventional control method. To cope with this challenge, an FIR-based active damping method is employed to compensate for the delay's adverse effect and expand the critical frequency. In this way, the system can remain stable irrespective of the grid impedance wide variations. Also, it is shown that the proposed control system can be used in grid-connected microgrids, where the interaction between inverters puts the whole system at the risk of instability. Analytical results show that using the proposed FIR filter, grid impedance variations and interaction between inverters never make the system unstable, since the phase of inverter output admittance is always lower than 90°. The capability of the control system is validated using analysis and experimental results in different case studies.

Appendix

PSO Parameters

Swarm size	500
Number of iterations	500
Inertia weight	1
Inertia weight damping ratio	0.995
Personal learning coefficient	2
Global learning coefficient	2

References

[1] S. Jayalath and M. Hanif, "Generalized *LCL*-filter design algorithm for grid-connected voltage-source inverter," *IEEE Trans. Ind. Electron.*, vol. 64, no. 3, pp. 1905–1915, Mar. 2017.

[2] Y. Han, M. Yang, H. Li, P. Yang, L. Xu, E. A. A. Coelho, and J. M. Guerrero "Modeling and stability analysis of *LCL*-type grid-connected inverters: A comprehensive overview," *IEEE Access*, vol. 7, pp. 114975-115001, 2019.

[3] R. Peña-Alzola, M. Liserre, F. Blaabjerg, R. Sebastián, J. Dannehl, and F. W. Fuchs, "Analysis of the passive damping losses in *LCL*-filter-based grid converters," *IEEE Trans. Power Electron.*, vol. 28, no. 6, pp. 2642-2646, Jun. 2013.

[4] J. Dannehl, C. Wessels, and F. W. Fuchs, "Filter-based active damping of voltage source converters with *LCL* filter," *IEEE Trans. Ind. Electron.*, vol. 58, no. 8, pp. 3623–3633, Aug. 2011.

[5] X. Wang, F. Blaabjerg and P. C. Loh, "Grid-current-feedback active damping for *LCL* resonance in grid-connected voltage-source converters," *IEEE Trans. Power Electron.*, vol. 31, no. 1, pp. 213-223, Jan. 2016.

[6] Y. Jia, J. Zhao, and X. Fu, "Direct grid current control of *LCL*-filtered grid-connected inverter mitigating grid voltage disturbance," *IEEE Trans. Power Electron.*, vol. 29, no. 3, pp. 1532–1541, Mar. 2014.

[7] T. Liu, J. Liu, Z. Liu, and Z. Liu, "A study of virtual resistor-based active damping alternatives for *LCL* resonance in grid-connected voltage source inverters," *IEEE Trans. Power Electron.*, vol. 35, no. 1, pp. 247–262, Jan. 2020.

[8] S. Y. Park, C. L. Chen, J. S. Lai, and S. R. Moon, "Admittance compensation in current loop control for a grid-tie *LCL* fuel cell inverter," *IEEE Trans. Power Electron.*, vol. 23, no. 4, pp. 1716–1723, Jul. 2008.

[9] D. Pan, X. Ruan, C. Bao, W. Li, and X. Wang, "Capacitor-current-feedback active damping with reduced computation delay for improving robustness of *LCL*-type grid-connected inverter," *IEEE Trans. Power Electron.*, vol. 29, no. 7, pp. 3414–3427, Jul. 2014.

[10] X. Ruan, X. Wang, D. Pan, D. Yang, W. I. Li, and C. Bao, "Resonance damping methods of *LCL* filter," in *Control Techniques for LCL-Type Grid-Connected Inverters*. Beijing, China: Springer, 2018, ch. 8, pp. 165–196.

[11] J. L. Agorreta, M. Borrega, J. López, and L. Marroyo, "Modeling and control of *N*-paralleled grid-connected inverters with *LCL* filter coupled due to grid impedance in PV plants," *IEEE Trans. Power Electron.*, vol. 26, no. 3, pp. 770-785, Mar. 2011.

[12] A. Akhavan, H. R. Mohammadi, and J. M. Guerrero, "Modeling and design of a multivariable control system for multi-paralleled grid-connected inverters with *LCL* filter," *Int J Electric Power Energy Syst.*, vol. 94, pp. 354–362, Jan. 2018.

[13] X. Wang, F. Blaabjerg, and P. C. Loh, "Virtual *RC* damping of *LCL*-filtered voltage source converters with extended selective harmonic compensation," *IEEE Trans. Power Electron.*, vol. 30, no. 9, pp. 4726–4737, Sep. 2015.

[14] Z. Xin, X. Wang, P. C. Loh, and F. Blaabjerg, "Grid-current-feedback control for *LCL*-filtered grid converters with enhanced stability," *IEEE Trans. Power Electron.*, vol. 32, no. 4, pp. 3216-3228, Apr. 2017.

[15] A. Akhavan, H. R. Mohammadi, J. C. Vasquez, and J. M. Guerrero, "Passivity-based design of plug-and-play current-controlled grid-connected inverters," *IEEE Trans. Power Electron*, vol. 35, no. 2, pp. 2135-2150, Feb. 2020.

[16] X. Li, X. W. Y. Geng, X. Yuan, C. Xia, and X. Zhang, "Wide damping region for *LCL*-type grid-connected inverter with an improved capacitor current- feedback method," *IEEE Trans. Power Electron.*, vol. 30, no. 9, pp. 5247–5259, Sep. 2015.

[17] V. Miskovic, V. Blasko, T. Jahns, A. Smith, C. Romenesko, "Observer-based active damping of *LCL* resonance in grid-connected voltage source converters" in *Proc. IEEE Energy Convers. Congr. Expo*., 2013, pp. 4850–4856.

[18] G. Escobar, P. Mattavelli, M. Hernandez-Gomez, and P. R. Martinez Rodriguez, "Filters with linear-phase properties for repetitive feedback," *IEEE Trans. Ind. Electron.*, vol. 61, no. 1, pp. 405–413, Jan. 2014.

[19] G. Escobar, M. Hernandez-Gomez, A. A. Valdez-Fernandez, M. Lopez-Sanchez, and G. A. Catzin-Contreras, "Implementation of a 6*n*±1 repetitive controller subject to fractional delays," *IEEE Trans. Ind. Electron.*, vol. 62, no. 1, pp. 444–452, Jan. 2015.

[20] S. Buso and P. Mattavelli, *Digital Control in Power Electronics*, San Rafael, CA, USA: Morgan & Claypool Publ., 2006.

[21] G. Escobar, P. Mattavelli, and M. F. Martinez-Montejano, "Modifications to repetitive-based controllers using FIR filters for practical implementation" in *Proc. 34th IEEE IECON*, Nov. 2–5, 2009, pp. 3246–3251.

[22] M. Clerc, *Particle Swarm Optimization*, Newport Beach, CA, USA: ISTE USA, 2006.

[23] K. E. Parsopoulos and M. N. Vrahatis, *Particle Swarm Optimization and Intelligence: Advances and Applications*, Hershey, PA, USA: Information Science Reference, 2010.

[24] C. Blum and D. Merkle, *Swarm intelligence: introduction and applications*, Berlin, Germany: Springer, 2008.

[25] C. Bao, X. Ruan, X. Wang, W. Li, D. Pan, and K. Weng, "Step-by-step controller design for *LCL*-type grid-connected inverter with capacitor-

current feedback active-damping," *IEEE Trans. Power Electron.*, vol. 29, no. 3, pp. 1239–1253, Mar. 2014.

[26] A. G. Yepes, A. Vidal, J. Malvar, O. López, and J. Doval-Gandoy, "Tuning method aimed at optimized settling time and overshoot for synchronous proportional-integral current control in electric machines," *IEEE Trans. Power Electron.*, vol. 29, no. 6, pp. 3041–3054, Jun. 2014.

[27] D. Pan, X. Ruan, X. Wang, F. Blaabjerg, X. Wang, Q. Zhou, "A highly robust single-loop current control scheme for grid-connected inverter with an improved *LCCL* filter configuration", *IEEE Trans. Power Electron.*, vol. 33, no. 10, pp. 8474−8487, Oct. 2018.

[28] D. G. Holmes, T. A. Lipo, B. P. McGrath, and W. Y. Kong, "Optimized design of stationary frame three phase AC current regulators," *IEEE Trans. Power Electron.*, vol. 24, no. 11, pp. 2417–2426, Nov. 2009.

[29] A. G. Yepes, F. D. Freijedo, J. Doval-Gandoy, O. Lopez, J. Malvar, Fernandez-Comesana, "Effects of discretization methods on the performance of resonant controllers", *IEEE Trans. Power Electron.*, vol. 25, no. 7, pp. 1692-1712, Jul. 2010.

[30] J. Sun, "Impedance-based stability criterion for grid-connected inverters," *IEEE Trans. Power Electron.*, vol. 26, no. 11, pp. 3075-3078, Nov. 2011.

Ali Akhavan (Member, IEEE) received the B.S., M.S., and Ph.D. degrees in electrical engineering from University of Kashan, Kashan, Iran in 2012, 2014, and 2019, respectively. Since August 2019, he has been with Aalborg University, Aalborg, Denmark, where he is currently a Postdoctoral Fellow with the Department of Energy Technology. His research interests include power electronics, modeling and control of grid-connected converters, stability analysis, and microgrid clusters.

Saeed Golestan (Senior Member, IEEE) received the B.Sc. degree from Shahid Chamran University of Ahvaz, Iran, in 2006, the M.Sc. degree from Amirkabir University of Technology, Tehran, Iran, in 2009, and the Ph.D. degree from Aalborg University, Aalborg, Denmark, in 2018, all in electrical engineering. He is currently an assistant professor at the Department of Energy Technology, Aalborg University, Aalborg, Denmark. His research interests include modeling, synchronization, and control of power electronic systems and microgrids.

Juan C. Vasquez (Senior Member, IEEE) received the B.S. degree in electronics engineering from the Autonomous University of Manizales, Manizales, Colombia, in 2004, and the Ph.D. degree in automatic control, robotics, and computer vision from BarcelonaTech-UPC, Spain, in 2009. He was Assistant Professor and Associate Professor with the Department of Energy Technology, Aalborg University, Denmark, in 2011 and 2014, respectively. In 2019, he became Professor in energy internet and microgrids. Currently, he is the Co-Director of the Villum Center for Research on Microgrids (CROM). He was a Visiting Scholar with the Center of Power Electronics Systems (CPES), Virginia Tech, U.S.A. and a Visiting Professor with Ritsumeikan University, Japan. He has published more than 450 journal papers in the field of microgrids, which in total are cited more than 19000 times. His current research interests include operation, advanced hierarchical and cooperative control, optimization and energy management applied to distributed generation in ac/dc microgrids, maritime microgrids, advanced metering infrastructures, and the integration of Internet of Things and energy Internet into the SmartGrid.

Josep M. Guerrero (Fellow, IEEE) received the B.S. degree in telecommunications engineering, the M.S. degree in electronics engineering, and the Ph.D. degree in power electronics from the Technical University of Catalonia, Barcelona, Spain, in 1997, 2000, and 2003, respectively. Since 2011, he has been a Full Professor with the Department of Energy Technology, Aalborg University, Aalborg, Denmark, where he is responsible for the Microgrid Research Program. From 2014, he has been a Chair Professor with Shandong University; from 2015, he has been a Distinguished Guest Professor with Hunan University; and from 2016, he has been a Visiting Professor Fellow with Aston University, Birmingham, U.K.; and a Guest Professor with the Nanjing University of Posts and Telecommunications, Nanjing, China. From 2019, he has been a Villum Investigator by The Villum Fonden, Søborg, Denmark, which supports the Center for Research on Microgrids (CROM), Aalborg University, being the founder and Director of the same center. His research interests include different microgrid aspects, including power electronics, distributed energy-storage systems, hierarchical and cooperative control, energy management systems, smart metering and the Internet of Things for ac–dc microgrid clusters and islanded minigrids. He has authored or coauthored more than 600 journal papers in the fields of microgrids and renewable energy systems, which are cited more than 50000 times. His research specially focuses on microgrid technologies applied to offshore wind, maritime microgrids for electrical ships, vessels, ferries and seaports, and space microgrids applied to nanosatellites and spacecrafts.

Chuan Xie (Senior Member, IEEE) received the B.S. degree in automation engineering from the University of Electronic Science and Technology of China (UESTC), Chengdu, China, in 2007, and the Ph.D. degree in power electronics from Zhejiang University, Hangzhou, China, in 2012. Since 2012, he has been a Lecturer with the School of Automation Engineering, UESTC, where he was promoted as an Associate Professor in 2019. From 2015 to 2016, he was a Visiting Scholar with the Department of Energy Technology, Aalborg University. His main research interests include digital control of power electronics, grid synchronization technology, distributed generation systems, microgrids, and power quality.